https://doi.org/10.5281/zenodo.14845153

Beitrag “Der Geothermiekongress DGK 2024”, 22. – 24. Oktober 2024 in Potsdam

SINDI DRILLING: Showcasing a Real time Drilling Hydraulics Simulation and Monitoring Tool Using a Recorded Rig Sensor Dataset

Wisam Sindi

Sindi Digital Energy Technologies UG, Germany

Topics: Commercial projects, operational experience

Keywords: Geothermal, Digitalization, Drilling Operations, Real-time Drilling Hydraulics Monitoring, API Recommended Practice 13D

Abstract

To integrate geothermal energy into the future energy portfolio, it is essential to reduce the technical and financial risks of drilling deep geothermal wells. This can be achieved using a tool that detects drilling problems such as plugged nozzles, cuttings accumulations, circulation loss, and well control issues.

A real time drilling rig hydraulics tool is presented to determine theoretical standpipe pressure (SPP), equivalent circulating density (ECD), annular cutting velocities, and flow regimes. The methodology uses a dynamic geometrical representation of the wellbore/drillstring system to simulate wellbore hydraulics in real time. The drilling fluid's rheology is modelled using Power-Law, Bingham-Plastic, and Herschel-Bulkley models according to API Recommended Practice 13D. The model adapts to changes in pump rate and drillstring movement by utilizing real time rig sensor data, including pump strokes, flow rate, and bit/hole depth.

The model was validated with 500 hours of historical rig sensor data from drilling four oil wells with water-based mud (WBM) and one deep-water High Pressure High Temperature (HPHT) well with synthetic-based mud, with drilled depths ranging from 3050 to 6000 m. It accurately predicted SPP for conventional drilling with WBM in both vertical and horizontal wellbores, with deviations of 0–10 bars. Short-term trends for measurements and predictions correlated well.

For the HPHT well, accuracy was lower, though trends were similar to those observed with WBM. This suggests that downhole temperature and pressure effects on mud shear stress should be considered. Special considerations allow the model to simulate specific drill string components (e.g., heavy weights, collars, mud motors, and tool joints) without needing detailed design specifications.

The calculated ECD along the wellbore enables the mitigation of losses and the prevention of influx. Moreover, the solution allows for the detection of plugged nozzles and insufficient rock cutting removal.

Having such a model helps reduce non-productive time by integrating it with monitoring and automation processes.

Introduction

Problem

Drilling operations have become increasingly challenging to perform in a cost-effective and safe manner, particularly in cases with (Ruggero Bertani, 2018):

- Physical limits, such as narrow ECD windows in shallow horizontal wells.
- Uncertainties related to pore and fracture pressures and potential over-pressurized zones.
- Challenging environments, such as deep water, high-pressure/high-temperature (HPHT), or supercritical conditions.
- Ineffective drilling processes due to issues like plugged nozzles, poor rock cuttings removal, and circulation loss.

Monitoring

In the framework of monitoring, rig sensor data are transferred to remote processing centers via standard interfaces and connected to mathematical models to calculate key operational parameters, e.g. surge pressure, SPP and ECD, in real time (Cayeux, Daireaux, Dvergsnes, & Sælevik, 2012). For instance the knowledge of the theoretical SPP in real time enables the drilling engineer to identify events of deterioration of the drilling process, in early stages, providing the chance to react and reduce unproductive rig time. Such situations include well control after taking a kick, stuck pipe, loss of circulation, BHA pack-off due the generation of cutting beds as result of insufficient hole cleaning, plugged bit nozzles (Rommetveit, Ødegård, Bjørkevoll, & Mike Herbert, 2009) and hole collapse (Chmela, Abrahmsen, & Haugen, 2014).

Automation

Automation of conventional drilling includes safe-guarding and safety triggering to optimize drilling. The aim of safeguarding is to system-control the machinery in such a way to ensure that certain operation parameters are kept between limits. For instance limiting the mud pump rate to keep the downhole pressure within limits that are determined from modelling, in real time.

Moreover, safety triggers are put in place to automatically react in abnormal situations, detected through deviation from parameter thresholds, derived from real time modelling. Beside prediction of key parameters, results of a matched model may serve to fill-in of sensor data in time and space. For example, to replace PWD when no mud pulse telemetry is possible, or to model ECD at the casing shoe when sensors are located much further towards BHA (Bjørkevoll, Daireaux, & Berg, 2015).

SINDI DRILLING Simulation Tool

A rig/wellbore drilling hydraulics monitoring tool is essential for detecting and mitigating drilling problems such as plugged nozzles, cuttings accumulation, and well control issues.

SINDI DRILLING is a simulation tool for real-time monitoring using rig sensor data, and "offline" job design calculations. The solution was developed based on practical experience and state-of-the-art science.

This tool prioritizes intuitive and user-friendly operation and is equipped with a graphical user interface (GUI) featuring dropdown menus for easy input and results visualization. Hydraulic key parameters ensuring a safe and efficient drilling process are calculated and analyzed against measurements (or thresholds), including standpipe pressure (SPP), equivalent circulating density (ECD), mud loading, cuttings velocity, surge and swab pressures, and wellbore in/out-flux.

The solution can also be used for offline wellbore hydraulics calculations, enabling design calculations during the planning phase. This process requires setting up the wellbore system, including the wellbore schematic, surface facility, drillstring tools, and the mud, using the provided GUI panels listed below.

1. Wellbore Schematic and Surface Facility
2. Drillstring Tools and Dynamic Hydraulics Fields
3. Mud Properties and Mud Motor
4. Offline Pressure Calculation
5. Real time Pressure Calculation
6. SPP, ECD, Slip, and Geometry vs. MD
7. Surge and Swab

To perform real-time wellbore hydraulics simulations, it is necessary to set up the wellbore system in the same way as for offline calculations, with the addition of connecting to a rig sensor data source (e.g., a database, historian, or cloud).

Below some of the GUI panels are presented.

Wellbore Schematic

As shown in Figure 1, the tool allows users to enter the wellbore schematic, which comprises sections such as the riser, casing, openhole, and drilling liner. All four sections can be used simultaneously.

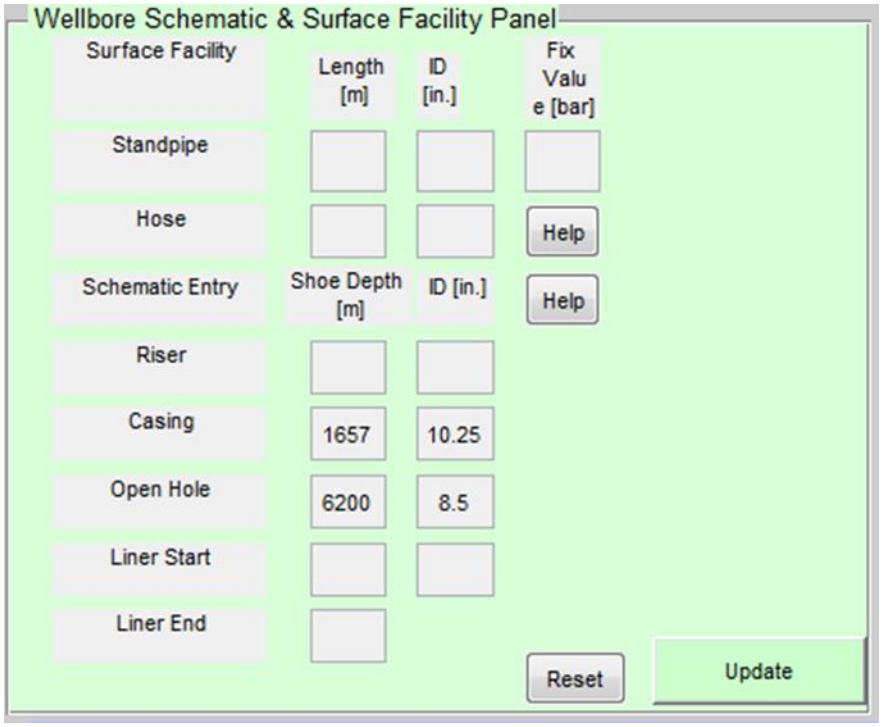

Figure 1 Wellbore Schematic & Surface Facility Panel.

Dynamic Hydraulics Fields

Figure 2 shows the calculation results instantly. For both offline calculations and full real-time simulation modes, drillstring tools and pressures are calculated and displayed dynamically. The last row displays the 'Dynamic Hydraulics Fields,' where the 'Sum of Dynamic Hydraulics' represents the total pressure losses along the entire drillstring. Adding the 'Sum of Dynamic Hydraulics' to the surface pressure losses yields the calculated SPP.

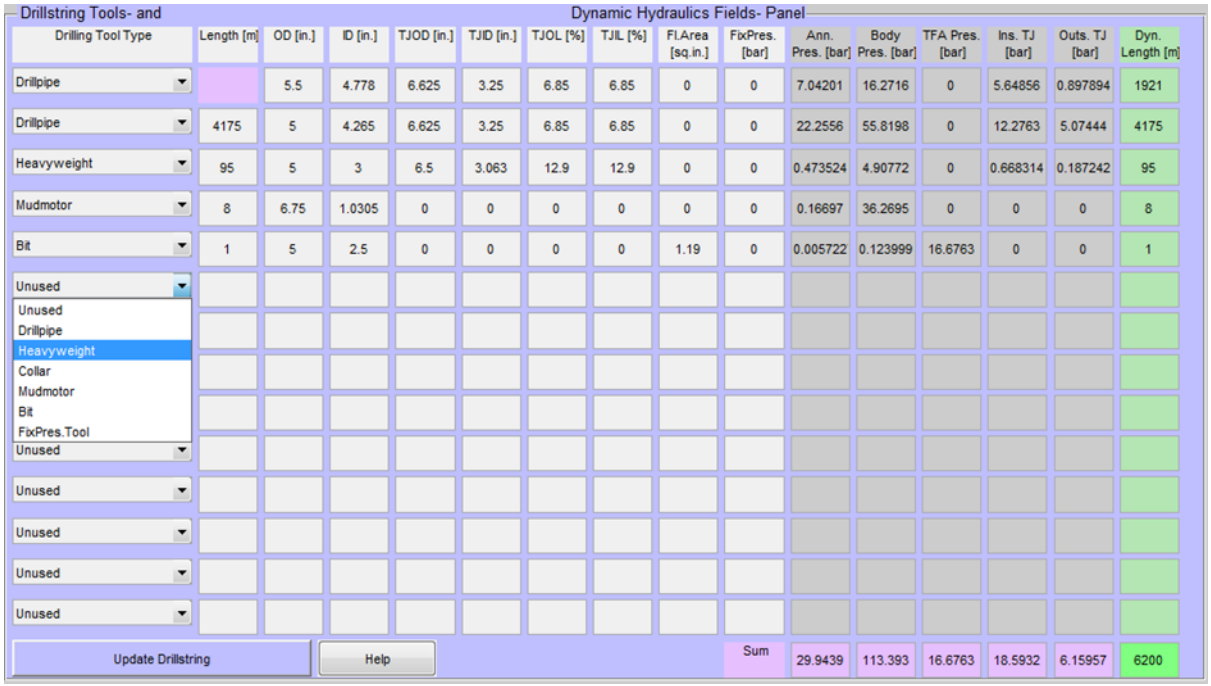

Figure 2 Drillstring Tools- and Dynamic Hydraulics Fields- Panel.

Offline Pressure Calculation Panel

This panel allows for data entry and displays calculated key parameters, including SPP, ECD, and mud density, as well as API cutting load and total flow area (TFA)-reduction SPP. The offline calculations panel is shown in Figure 3.

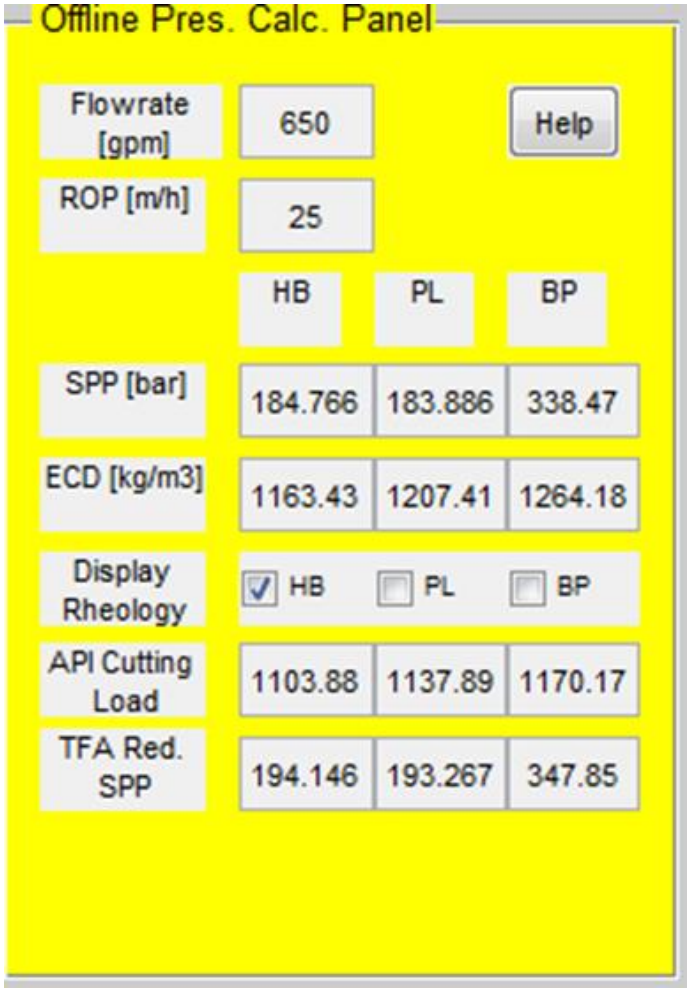

Figure 3 Offline Pressure Calculations Panel.

Real time Pressure Calculation Panel

This panel allows for data entry and displays measured and real-time calculated parameters. For the given field case, these parameters include real-time flow rate, rate of penetration (ROP), and standpipe pressure (SPP) at the current time step. The real-time calculations panel is shown in Figure 4.

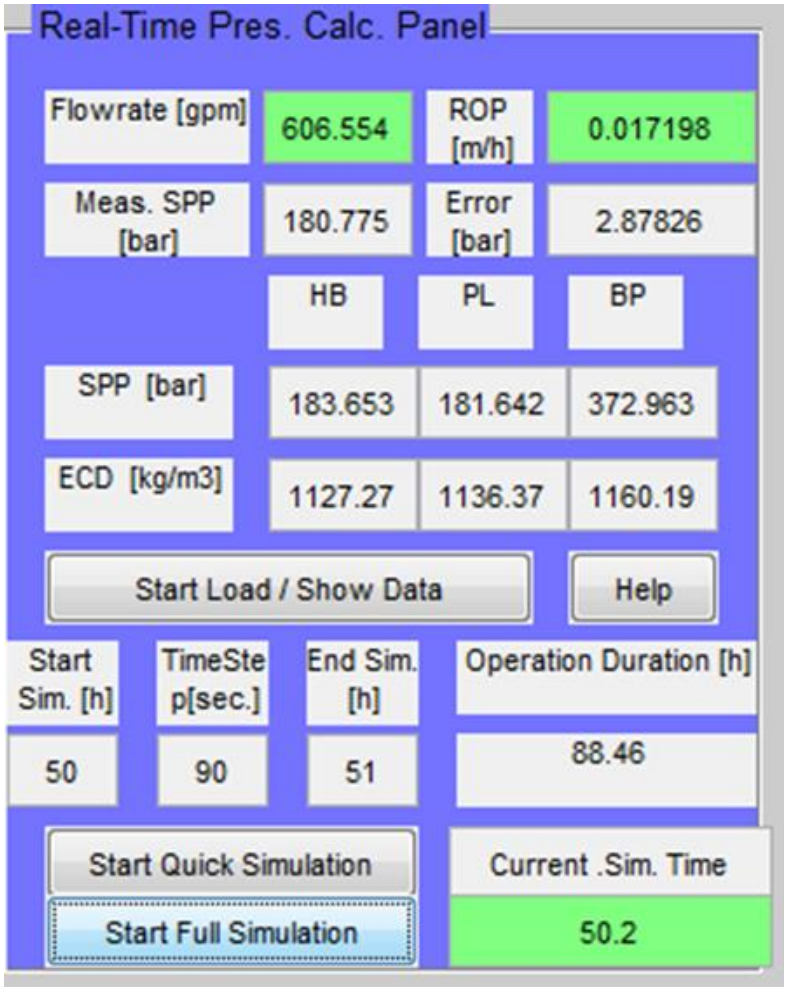

Figure 4 Real time Pressure Calculations Panel

Methodology

Wellbore hydraulics are calculated utilizing a single viscometer measurement performed at standard conditions. The fann viscometer readings are obtained as per (API RP 13D, 2010).

Figure 5 shows one generated idealized geometric representation of the wellbore, along the calculated hydraulic parameters.

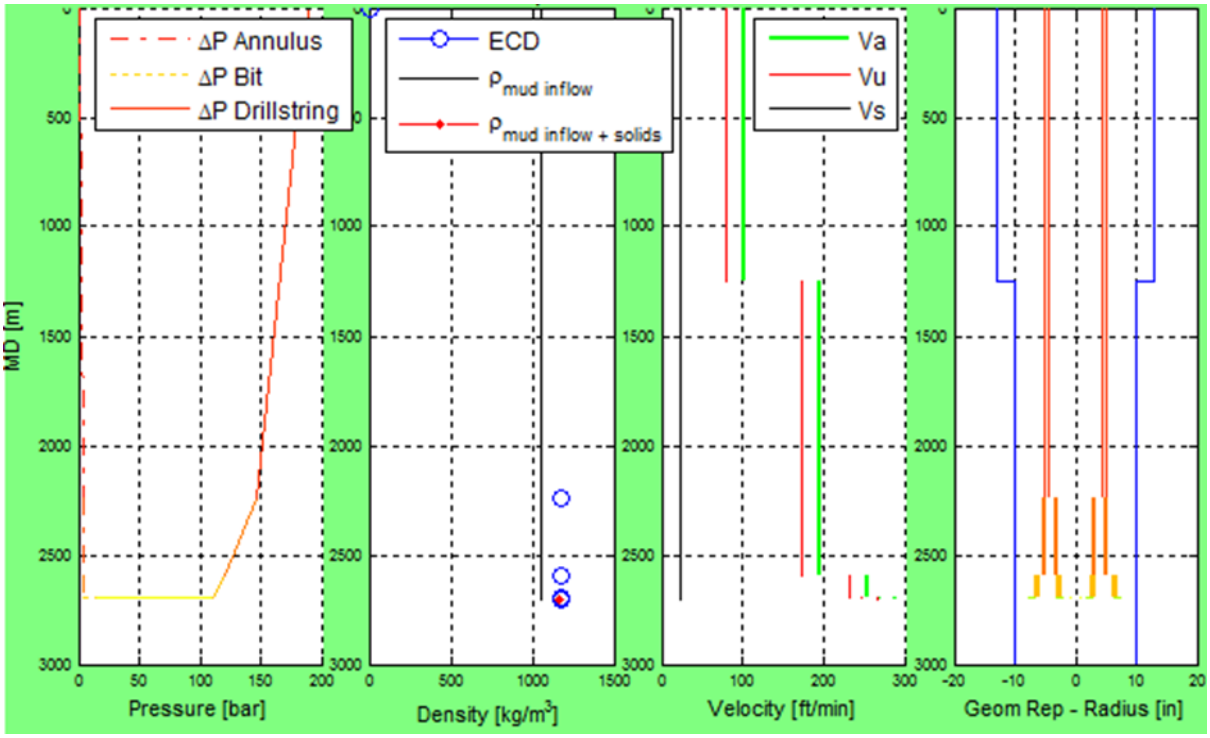

Figure 5 Calculated pressure losses, densities and velocities in the annulus, and idealized geometric representation of the wellbore-drillstring system (Radial dimensions of the tools are not to scale).

Rheology

Introduction to rheology - Shear stress, shear rate and their relationship

Force per unit area required to maintain a fluid flowrate is the shear stress. Shear rate is the rate of change of flow velocity as function of the distance to the pipe wall and is a velocity gradient, in inverse second units. Viscosity is the ratio of the shear stress to shear rate.

The drilling fluids utilized in this work are shear thinning as they generate less viscosity at higher shear rates than at lower shear rates. Like most of the drilling fluids, they do not show directly proportionality between shear stress and shear rate, and are called non-Newtonian.

Rheological models are mathematical functions or curve fits that describe the relationship between shear rate and shear stress of a fluid.

Rheology models

The Bingham Plastic rheological model (BP) developed by (Bingham, 1922) takes account for the minimum required yield stress to initiate fluid movement, but it depicts a constant viscosity

regardless of the shear rate. Therefore it overtimes the viscosity of shear-thinning fluids at high shear rates and vice versa (Eq. 1).

Eq. 1

$$\tau = \tau_y + \dot{\gamma}\,\mu_p$$

The Power Law rheological model (Dodge, 1959) describes fluid properties via two parameters, the consistency index (K) and, the flow behavior index (n). The index K describes the thickness of the fluid and is analogous to the apparent viscosity (μ_a). Large K values indicate a high fluid thickness, whereas n indicates the intensity of Non-Newtonian behavior.

The shortcoming of the Power Law Model is its inability to describe shear stress and rate relation at low and medium shear rates (Eq. 2).

Eq. 2

$$\tau = K\,\dot{\gamma}^n$$

The Herschel-Bulkley (H.-B.) or Yield Power Law rheological model was first presented by (Herschel & Bulkley, August 1926), it combines the theoretical and practical aspects of both the Bingham plastic and Power Law models. However, the complexity of the solution for the model's three parameters n, K, and τ_0 and lack of mud hydraulics equations made its application impossible, until made available by (Pilehvari, Campos, & Hemphill, 1993) and (Reed & Pilehvari, 1993).

For fluids having a yield stress, n and K will be different when determined by the models H.-B. and PL. The parameter τ_0 is the fluid's yield stress at zero shear rate, i.e. zero viscometer rpm. In theory τ_0 is identical to τ_y of the BP model, though its calculated value is different.

In contrast to PL, H.-B. considers τ_y. In special cases, the H.-B. becomes the BP when n = 1, and it becomes the PL model when $\tau_0 = 0$ (Eq. 3).

Eq. 3

$$\tau = \tau_0 + K\,\dot{\gamma}^n$$

Figure 6 depicts the rheology models H.-B., PL and BP (Reed & Pilehvari, 1993).

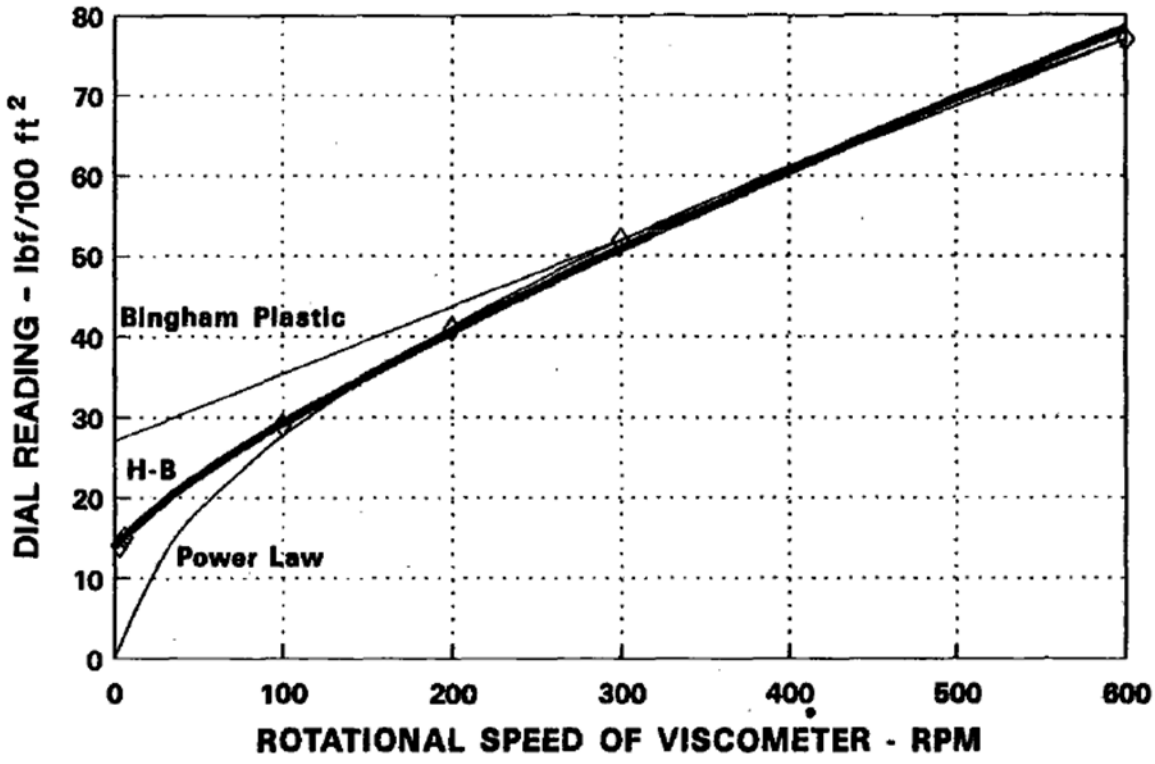

Figure 6 Rheological models and viscometer readings for a typical bentonite water based mud. Source: (Reed & Pilehvari, 1993).

Mud properties are obtained and deployed using the BP, PL and H.-B. rheology models, as suggested in (API RP 13D, 2010).

Field cases and modelling results

Specifications of the Modelled Wellbores

The developed model was applied on recorded rig sensor data pertaining to drilling of the intermediate or the production section of five wellbores, all using a rotary steering system (RSS). One was a vertical HPHT using OBM. The other 4 wellbores were conventionally drilled using WBM, including a horizontal and 3 vertical ones. Figure 12 (in the appendix) shows an entire raw dataset of a field case.

Table 1 and Table 2 provide descriptions of the wellbores with regards to the utilized drilling mud, the wellbore schematics, and the drillstring components (only those actually used by the model).

Table 1 Drilling muds utilized in the field cases

	Well-1	Well-2	Well-3	Well-4	Well-5
Mud Base	WBM	WBM	SBM	WBM	WBM
Mud Type	Ploymer	KCL-Polymer	Polymer	K2CO3-Polymer	K2CO3-Glycol
θ3 [lbf/100 ft²]	7	6	7	20	3

Θ6 [lbf/100 ft^2]	8.5	8	8	21	4
Θ300 [lbf/100 ft^2]	32	48	36	86	50
Θ600 [lbf/100 ft^2]	40	70	58	140	77
PV [cP]	8	22	22	54	27
YP [lbf/100 ft^2]	24	26	14	32	23
LSYP [lbf/100 ft^2]	5.5	4	6	19	2
HB K' [lbf s^n/ft^2]	2.47	1.15	0.21	0.33	0.62
HB n' [-]	0.38	0.58	0.79	0.852	0.88
PL K [lbf s^n/ft^2]	4.30	1.61	0.49	1.075	1.02
PL n [-]	0.32	0.54	0.69	0.702	0.62
Gel Strength 10sec/10min [Pa]	5.3 / 5.8	6 / 8	5.3 / 13.4	9/44	4/5
Density [kg/m3]	1070	1320	1370	1550	1160
Oil [vol%]	0	0	64	N/A	N/A
Water [vol%]	92	82	18.5	N/A	N/A
Solids [vol%]	6	18	17.5	11.6	N/A
Lubricant [vol%]	2	0	0	N/A	N/A
Sample Point	Flowline & Active Pit	Sample Depth 2840 m RT	Flowline & Active Pit	Active Silo	Active Silo

Table 2 Wellbore schematic, modeled depth-interval and operation-duration of the field cases

	Well-1	**Well-2**	**Well-3**	**Well-4**	**Well-5**
Mud Base	WBM	WBM	OBM	WBM	WBM
Riser Deph [m]/ ID [in]	-	-	2304/26	-	-
Csg Depth [m]/ Dia [in]	1660/10.3	1575/13.4	3305/19.5	2960/9.625	4850/7
OH Target ID [in]	8.5	10.6	18.1	8 3/8	5.875
Modelling MD Hole Start [m]	4050	2690	5350	2975	5050
Modelling MD Hole End [m]	6000	3050	6000	4160	5340
Modelling Drilled MD	1950	360	650	1185	290
Operation Duration [h]	230	91	15	45	162
Well Design	Horizontal, Conventional	Vertical, Conventional	Vertical, HTHP	Vertical until 3960, then slanted	Vertical until 3550, then sidetrack w/ const incl 22

The rheograms in Figure 7 illustrate that all muds utilized in this work are non-Newtonian and exhibit shear thinning behavior. This is also indicated by the 600 rpm viscometer readings being less than twice than at 300 rpm.

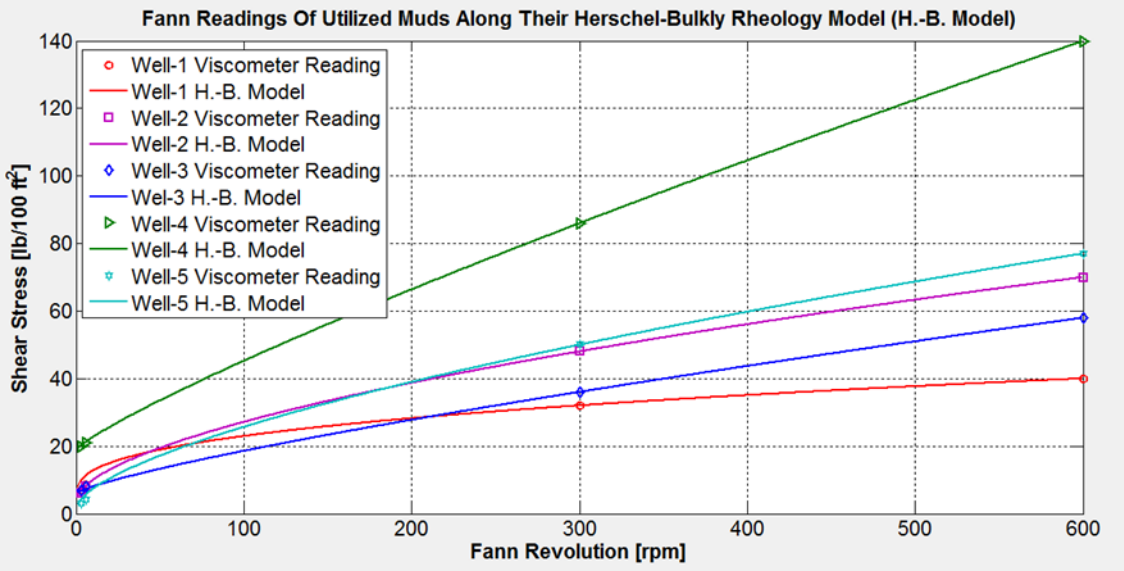

Figure 7 Rheograms of the shear thinning non-Newtonian drilling muds utilized in the field cases.

Figure 8 shows the resulting modelled SPP of 5 hours of operation, during which alternating on- and off-bottom situations occur, including making connections and downlinking operations. It shows that during off-bottom operation, the modelled pressure losses exceed the measured values. This is because the differential pressure pertaining to the maximum output power was used for calculation utilizing an equivalent internal diameter method.

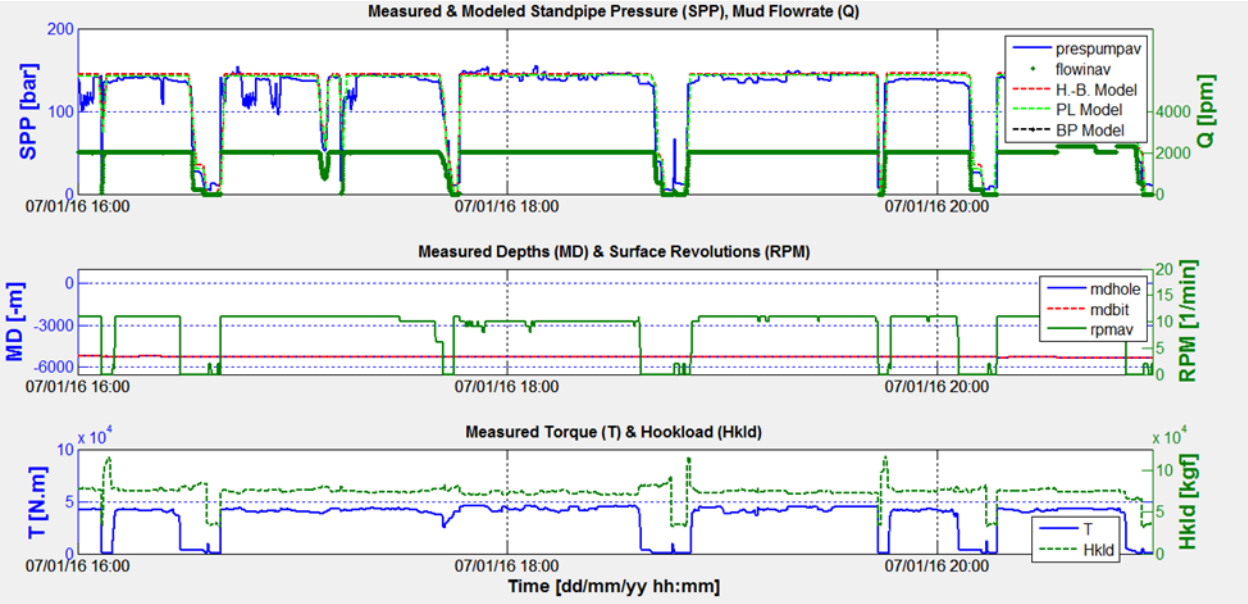

Figure 8 Measured and modeled SPP for 5 hours of operation, including alternating on-bottom and off-bottom operations, making connections and downlinking, for field case Well-1.

Modelling result of SPP

For field case Well-2, Figure 9 shows the modelled and measured SPP, and the prediction error of the model, for all three rheology models, along with a part of the sensor data.

For this modelling case, a time step of 450 seconds was used to model the 90 hours of operation (i.e. the data set at every other 450th second is modelled).

The results are obtained after an elapsed time of approximately two minutes and are considered representative for the whole data set.

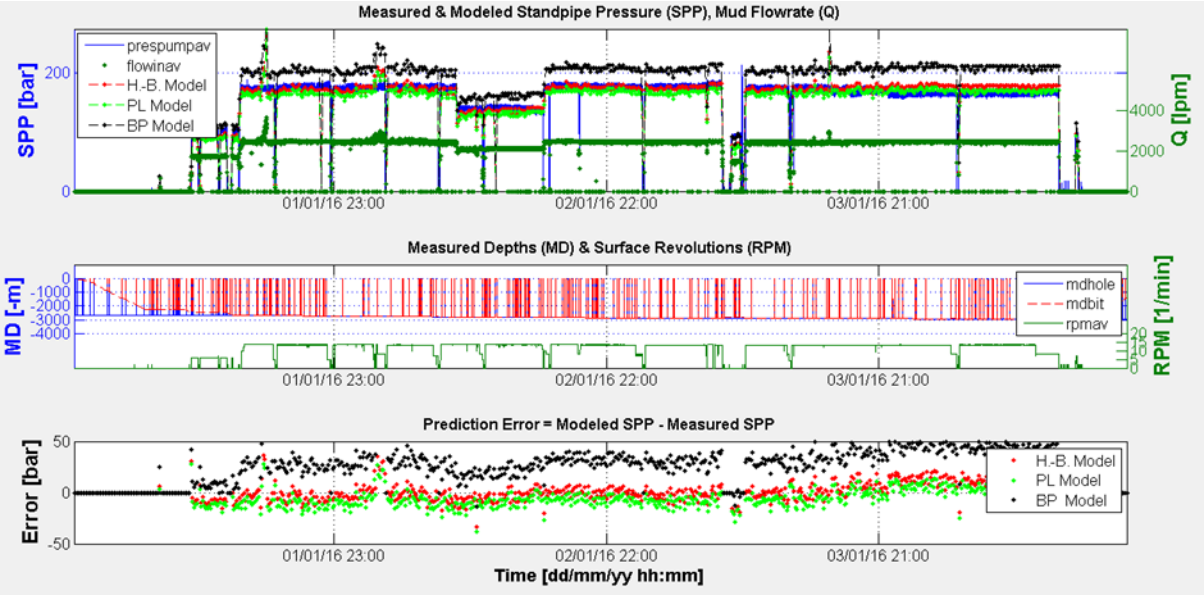

Figure 9 Measured and modelled SPP and the model-prediction error for all 3 rheologies, for field case Well-2.

Figure 10 depicts the prediction error histogram for the H.-B. model for Well-2. As can be seen, the frequency of the error follows approximately a normal distribution. Consequently, it can be assumed that the error is mostly randomly and there is no systematic bias. For all muds the distribution has a similar shape. For WBM‘s the mean is roughly at 0. For the OBM, the mean is shifted by 37.4 bar, indicating a conceptual error. The outliers are due to erratic sensor data.

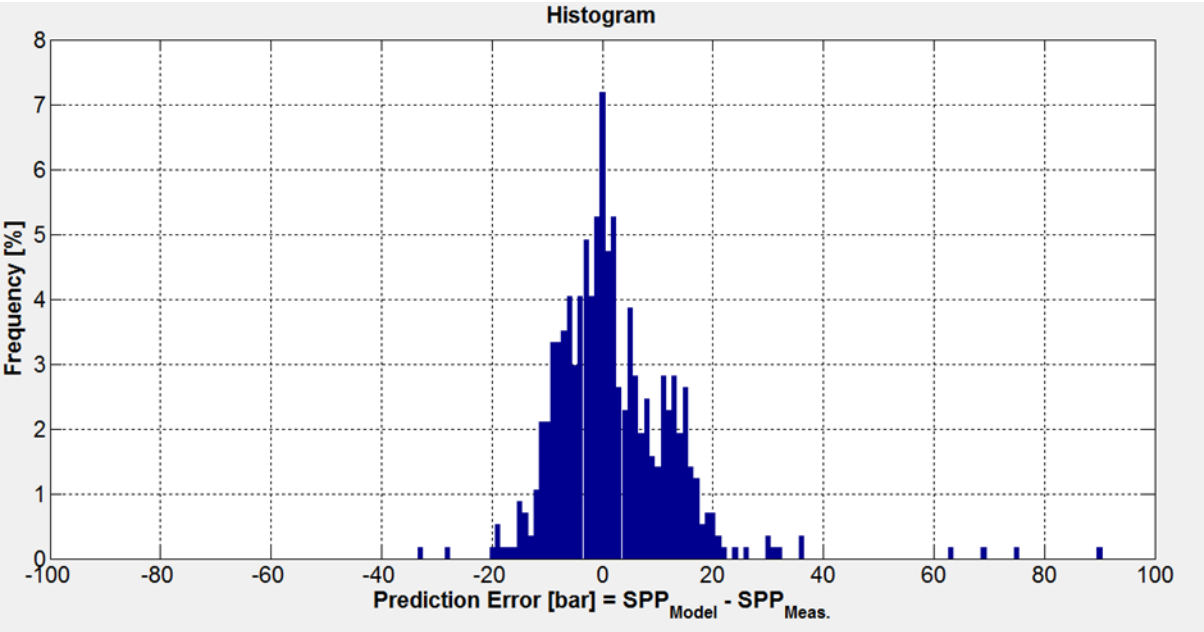

Figure 10 Histogram for model-prediction error for H.-B. for field case Well-2.

Table 3 shows the mean, median and standard deviation of the prediction error, in absolute numbers.

Since, for engineering purposes the absolute values are important, it was decided to calculate the prediction error statistics in absolute.

The prediction error is defined by Eq. 4, in units bar.

Eq. 4

$$Prediction\ Error = |SPP_{Model} - SPP_{Measured}|$$

Table 3 Mean, median and the standard deviation of the modeling results for all 5 field cases

Well	Error [bar]	H.-B.	PL	BP
Well-1 (Conventional, WBM)	Mean	9.8	8.3	138.1
	Med	7.4	5.8	161.3
	Std	10.2	9.6	91.4
Well-2 (Conventional, WBM)	Mean	6.8	8.0	26.5
	Med	4.2	6.7	28.8
	Std	12.5	12.2	19.6
Well-3 (HPHT, OBM)	Mean	37.4	48.5	16.8
	Med	55.2	76.0	18.7
	Std	28.0	37.5	10.8
Well-4 (Conventional, WBM)	Mean	8.5	20.8	44.0
	Med	6.8	20.2	44.8
	Std	8.7	10.2	12.2
Well-5 (Conventional, WBM)	Mean	8.2	7.9	77.6
	Med	6.2	4.1	77.7
	Std	8.6	10.2	18.6

Discussion, Conclusion & Future Work

Discussion

For field case Well-2, Figure 11 shows a shear stress versus shear rate chart along the actual viscometer readings, and the calculated effective viscosities pertaining to each of the rheology models. To ease the comparison, for both graphs the velocity gradient i.e. the shear rate was converted from inverse second to inverse minute units.

The BP model will overestimate the viscosity at high shear rates for WBM. This reflects the results of the SPP modelling. The BP-column in Table 3 shows the large errors.

Consequently, pressure losses are overestimated at high flowrates inside the drillstring, and vice versa in the annulus.

Moreover, since for this mud the PL index n = 0.54, which is closer to 1 than 0, the solution of PL is close to the solution of H.-B., but farther from BP rheological model.

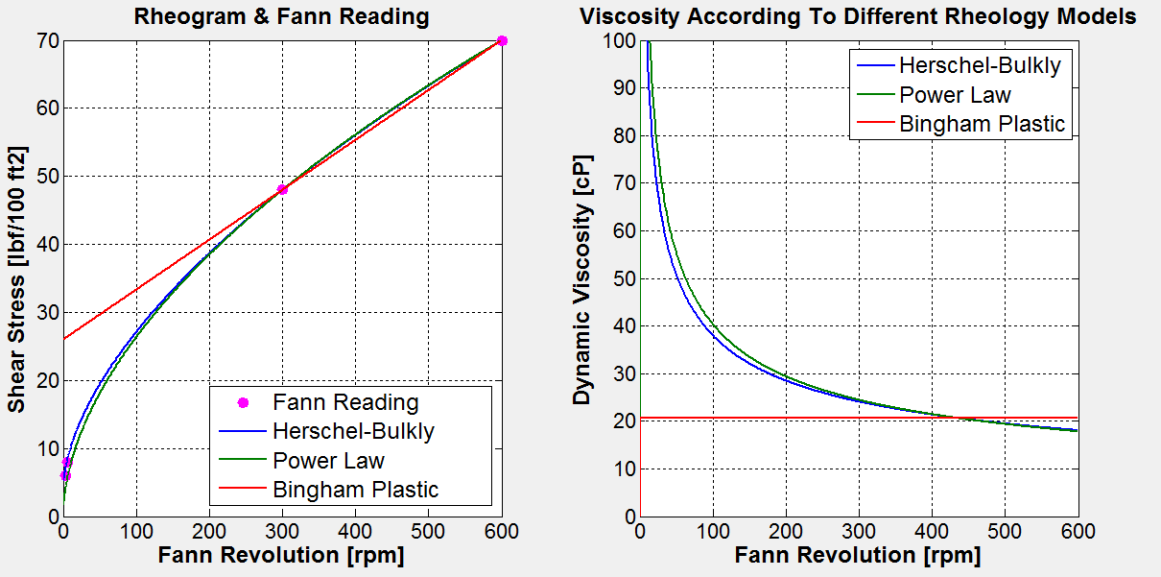

Figure 11 Shear stress vs shear rate, actual viscometer dial readings, and calculated effective viscosities, for field case Well-2.

Conclusion

Deployment of the developed solution on recorded rig surface sensor data for conventional drilling using water-based mud, has shown that prediction of the SPP within a mean deviation of 10 bars is possible.

One set of viscometer readings is sufficient for multiple subsequent days of drilling operations, in case no large mud behavior changing events occur.

It was shown that in wellbore hydraulics modelling some well-justified simplifications can significantly reduce computation efforts and input data need, without compromising too much with accuracy.

Based on the results, it can be confidently concluded that this solution can help reduce non-productive time and costs by detecting drilling problems at the onset such as:

- Formation fluids' influx, outflux (loss of circulation) by monitoring the theoretical real-time ECD along the wellbore.
- Drillstring pack-off due to poor rock cutting removal by monitoring the theoretical real-time annular cutting velocities.
- Plugged nozzles by monitoring the theoretical real-time TFA-reduced SPP

Future Work

Future work includes additional calculations to improve decision-making confidence based on the tool, such as:

- Torque and Drag (TaD) calculations to identify mechanical issues, such as monitoring drill string loads and preventing stuck pipe.
- Transient material balance for a more accurate description of wellbore fluid volume to address influx (kick) and outflux (loss of circulation) and to determine fluid properties.
- Managed Pressure Drilling (MPD) parameters to control ECD and downhole pressure at desired values (above pore pressure and below fracture pressure) to prevent drilling fluid loss or formation fluid influx.
- Accounting for pressure and temperature effects on drilling fluid (mud) properties, including volume expansion and viscosity changes

Nomenclature

Rheology

μ_a = Apparent viscosity, cP

μ_p = Plastic viscosity, cP

τ_0 = Yield stress at zero shear rate, lbf/100 ft^2

τ_y = Yield stress, lbf/100 ft^2

τ = Shear stress, lbf/100 ft^2

$\dot{\gamma}$ = Shear rate, 1/min

K = Consistency index, lbf s^n/100 ft^2

K = Tooljoint pressure loss coefficient, dimensionless

n = Flow behavior index, dimensionless

θ_x = Viscometer reading at x rpm, $x \in \{3, 6, 300, 600\}$

Hydraulics

BHA = Bottomhole assembly

d_{hyd} = Hydraulic diameter of annular conduit, in

d_i = Inner diameter of drillstring component, in

c = Instantaneous (cutting) solids concentration in the annulus, fraction

DC = Drillcollar

DP = Drillpipe

ECD = Equivalent circulating density, lbm/gal

ESD_a = Equivalent static density in the annulus, lbm/gal

HW = Heavywight

ID = Internal diameter, in

N_{Re} = Reynolds number, dimesionless

OBM = Oil (synthetic) based mud

OD = External diameter, in

P_a = Annulus pressure losses, bar

P_b = Bit pressure loss, dar

P_c = Casing back pressure, bar

P_{cl} = Choke line pressure loss, bar

PDM = Positive displacement motor (downhole mudmotor)

P_{ds} = Drillstring pressure losses, bar

P_{dt} = Downhole tools pressure losses, bar

P_{ha} = Annular hydrostatic pressure, bar

P_{hd} = Drillstring hydrostatic pressure, bar

P_{sc} = Surface connections pressure losses, bar

PWD = Pressure while drilling

Q = Flowrate, gal/min or gpm

ROP = Rate of penetration, ft/h

SPP = Standpipe pressure, bar

TFA = Total flow area, in^2

WBM = Water-based mud

ρ = Mud density inside the drillstring, lbm/gal or kg/m^3

ρ_a = Fluid density in annulus (local), lbm/gal

ρ_c = Density of the cuttings, g/cm^3

ρ_s = Drilling fluid density at surface, lbm/gal

Bibliography

API RP 13D. (2010). *Recommended Practice 13D, Rheology and Hydraulics of Oil-Well Drilling Fluids*. Washington DC: API.

Bingham, E. C. (1922). *Fluidity and Plasticity, page 219*. New York: McGraw-Hill.

Bjørkevoll, K. S., Daireaux, B., & Berg, P. C. (2015). Possibilities, Limitations and Pitfalls in Using Real-Time Well Flow Models During Drilling Operations. Society of Petroleum Engineers. doi:10.2118/173858-MS.

Cayeux, E., Daireaux, B., Dvergsnes, E., & Sælevik, G. (2012). Early Symptom Detection on the Basis of Real-Time Evaluation of Downhole Conditions: Principles and Results From Several North Sea Drilling Operations. Society of Petroleum Engineers. doi:10.2118/150422-PA.

Chmela, B., Abrahmsen, E., & Haugen, J. (2014). Prevention of Drilling Problems Using Real-Time Symptom Detection and Physical Models. Offshore Technology Conference. doi:10.4043/25460-MS.

Dodge, D. W. (1959). Turbulent Flow of Non-Newtonian Systems.

Herschel, W., & Bulkley, R. (August 1926). Konsistenzmessungen von Gummi-Benzollösungen. *Article Kolloid-Zeitschrift*, Volume 39, Issue 4, pp 291-300,.

Mathis, W., Thonhauser, G., Wallnoefer, G., & Ettl, J. (2007). Use of Real-Time Rig-Sensor Data To Improve Daily Drilling Reporting, Benchmarking, and Planning—A Case Study. Society of Petroleum Engineers. doi:10.2118/99880-PA.

Pilehvari, A., Campos, W., & Hemphill, T. (1993). Yield-Power Law Model More Accurately Predicts Mud Rheology. *Oil and Gas Journal*.

Reed, T. D., & Pilehvari, A. A. (1993). A New Model for Laminar, Transitional, and Turbulent Flow of Drilling Muds. . Society of Petroleum Engineers. doi:10.2118/25456-MS.

Rommetveit, R., Ødegård, S., Bjørkevoll, K., & Mike Herbert, C. N. (2009). Real-time monitoring, simulation, 3D visualization. . (pp. 47-52.). OIL WORLD - Drilling Technology.

Ruggero Bertani, H. B. (2018). *The First Results of the DESCRAMBLE Project.* Conference: 43rd Workshop on Geothermal Reservoir EngineeringAt: Stanford University, Stanford, California.

Todorov, D., & Thonhauser, G. (2014). Hydraulic Monitoring and Well Control Event Detection Using Model Based Analysis. Offshore Technology Conference. doi:10.4043/24803-MS.

Table of Figures

Figure 1 Wellbore Schematic & Surface Facility Panel. 4
Figure 2 Drillstring Tools- and Dynamic Hydraulics Fields- Panel. 4
Figure 3 Offline Pressure Calculations Panel. 5
Figure 4 Real time Pressure Calculations Panel 6
Figure 5 Calculated pressure losses, densities and velocities in the annulus, and idealized geometric representation of the wellbore-drillstring system (Radial dimensions of the tools are not to scale). 7
Figure 6 Rheological models and viscometer readings for a typical bentonite water based mud. Source: (Reed & Pilehvari, 1993). 9
Figure 7 Rheograms of the shear thinning non-Newtonian drilling muds utilized in the field cases. 11
Figure 8 Measured and modeled SPP for 5 hours of operation, including alternating on-bottom and off-bottom operations, making connections and downlinking, for field case Well-1. 11
Figure 9 Measured and modelled SPP and the model-prediction error for all 3 rheologies, for field case Well-2. 12
Figure 10 Histogram for model-prediction error for H.-B. for field case Well-2. 12
Figure 11 Shear stress vs shear rate, actual viscometer dial readings, and calculated effective viscosities, for field case Well-2. 14
Figure 12 Rig surface sensor measurement data of field case Well-2. 19
Figure 13 Tool Appearance while Full Real time calculation. 20

Table of Tables

Table 1 Drilling muds utilized in the field cases 9

Table 2 Wellbore schematic, modeled depth-interval and operation-duration of the field cases 10
Table 3 Mean, median and the standard deviation of the modeling results for all 5 field cases . 13

Appendix

Real time input rig sensor data

For the purpose of illustration, rig sensor data of one wellbore are shown. Figure 12 depicts the sensor measurements for field case Well-2.

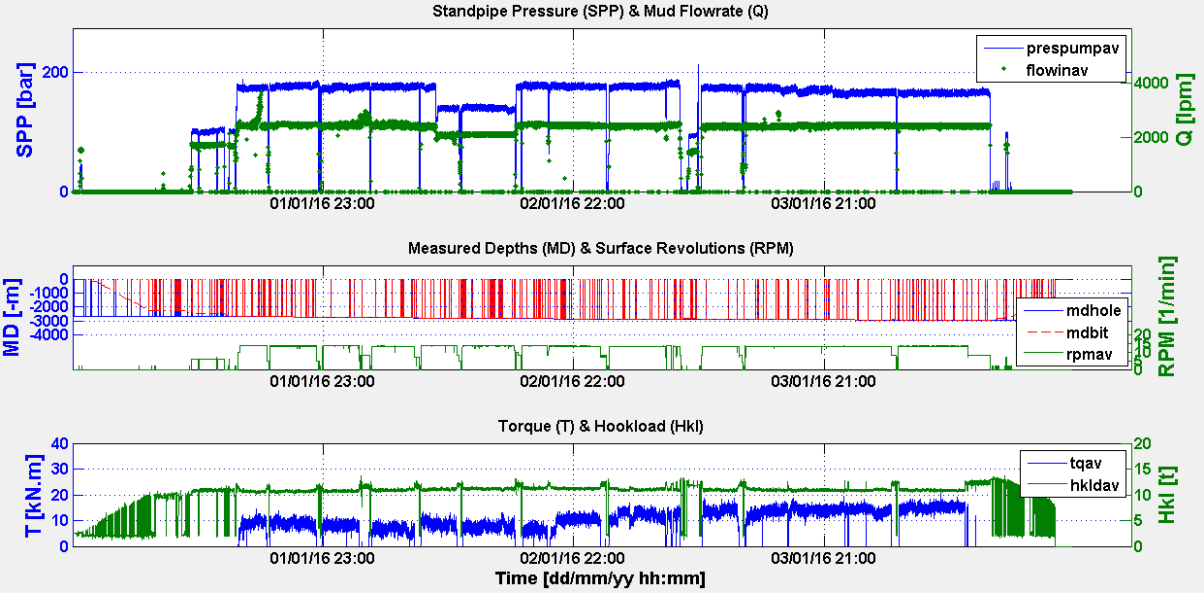

Figure 12 Rig surface sensor measurement data of field case Well-2.

Tool Appearance

Figure 13 shows the GUI in its entirety.

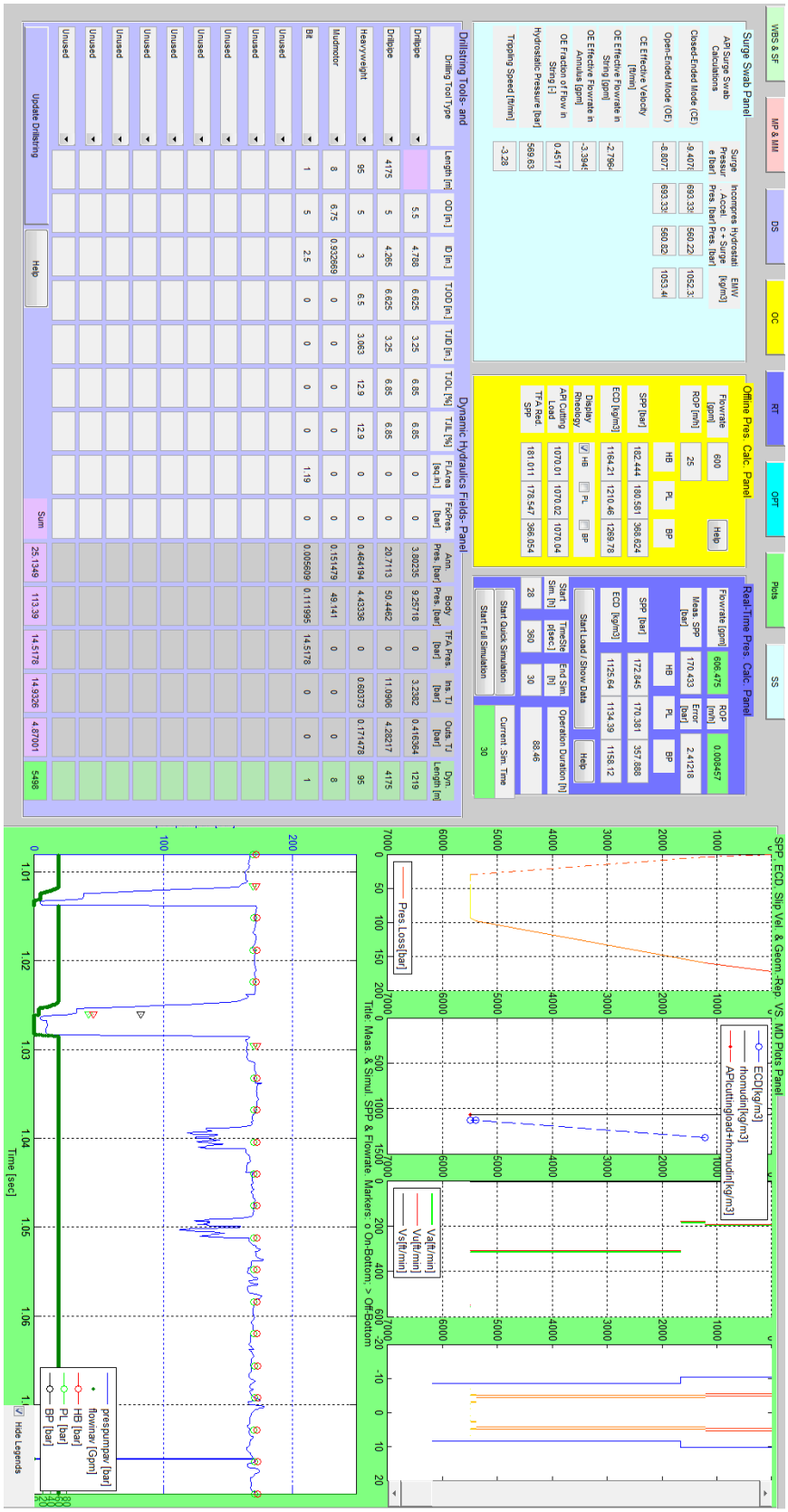

Figure 13 Tool Appearance while Full Real time calculation.

Sindi Digital Energy Technologies UG (haftungsbeschränkt)

Wisam Sindi, Managing Director

Ziegelhäuser Landstr. 55, 69120 Heidelberg, Germany

wisam.sindi@sindi-det.com